UCRL-JRNL-213654

LAWRENCE
LIVERMORE
NATIONAL
LABORATORY

Overview of ignition conditions and gain curves for the fast ignitor

S. Atzeni, M.Tabak

July 18, 2005

Plasma Physics and Controlled Fusion

Disclaimer

Overview of ignition conditions and gain curves for the fast ignitor

Stefano Atzeni†‡ and Max Tabak‡

† Dipartimento di Energetica, Università di Roma "La Sapienza" and INFM, Italy
‡ Lawrence Livermore National Laboratory, Livermore, California, U. S. A.

Abstract. Fast ignited inertially confined fusion targets have potentials for high gain at moderate laser energy. Gain estimates are based on simulations of separate aspects of target evolution and on gain models, and depend critically on ignition requirements and assumptions concerning coupling of the igniting beam to the compressed fuel. In this paper, we review and discuss ignition requirements, burn studies, and gain models. We present selected gain results, illustrating the dependence of the gain on the parameters of the ignition beam. We discuss the requirements for large very large gain, as well as for substantial gain at small driver energy.

Submitted to: *Plasma Phys. Control. Fusion*

1. Introduction

Fast ignition is an approach to inertial confinement fusion (ICF) in which fuel compression and ignition are separate processes [1]. The ignition hot spot is created in the precompressed fuel by an ultra-intense source, delivering energy as fast as the convergence of the stagnating flow in conventional ICF. In the original concept [1], the hot spot is created by relativistic electrons produced in ultra-intense laser-plasma interaction. A variant of the scheme uses laser-accelerated protons [2]. Intense heavy-ion beams [3, 4] and macroparticles [3] have also been proposed.

Fast ignitors have potentials for substantial advantages over conventional ICF: flexibility in compression drivers, higher gain and lower driver energy (and cost), lower susceptibility to hydrodynamic instabilities. The price to be paid is the need for coupling an ultra-intense energy source to the compressed fuel. Progress in ten years of fast-ignitor research has been reviewed in Ref. [5]. Pedagogical [6] and detailed [7] introductions have recently been published.

Fast ignition performance prediction are summarized by gain curves (e.g. [1, 3, 8, 9, 10] based on gain models incorporating theoretical concepts, simulation results, and extrapolation of present experimental results. Such models are also used to plan future experimental activity (e.g. see [9]).

‡ To whom correspondence should be addressed (stefano.atzeni@uniroma1.it)

In this paper, we briefly review gain models and a few underlying key issues. The presentation also includes new results on ignition and fuel burn. The target gain, i. e. the ratio of the released fusion energy to the total driver energy E can be written as

$$G = \frac{M_{\rm DT}\Phi Q_{\rm DT}}{E_{\rm c}^{\rm driver} + E_{\rm ig}^{\rm driver}}. \qquad (1)$$

Here $M_{\rm DT}$ is the mass of the DT fuel, $Q_{\rm DT} = 340$ MJ/mg is the DT yield, Φ is the fraction of burned fuel, and the total driver energy has been written as the sum of the energy $E_{\rm c}^{\rm driver}$ delivered by the compression driver, and of the energy $E_{\rm ig}^{\rm driver}$ of the ignition driver. As in any ICF scheme, the absorbed fraction $\eta_{\rm a}$ of the compression driver energy drives fuel compression to the final stagnation density ρ. The ignition hot spot is created by the fraction $\eta_{\rm ig}$ of the ignition driver energy actually coupled to the dense fuel.

Key ingredients of fast ignitor gain models are then the ignition requirements and the coupling efficiency $\eta_{\rm ig}$. Evaluation of the burn fraction Φ and of the compression energy is common to other ICF schemes, but some specific aspects (e.g. burn efficiency for non symmetric ignition, implosion schemes for isochoric compression, schemes for conically guided implosion) also deserve specific investigation.

In the next sections we discuss beam requirements for ignition, burn fraction, and gain computations, respectively.

2. Ignition conditions

Ignition requirements have been studied by numerical simulation. Their physical basis and scaling follow from a very simple hot spot model. Ignition of a uniform-density (isochoric) DT assembly requires a hot spot with [11]

$$H_{\rm h} = \rho r_{\rm h} = 0.5 \ {\rm g/cm}^2, \qquad (2)$$

$$T_{\rm h} = 12 \ {\rm keV}, \qquad (3)$$

where $H_{\rm h}$ is the confinement parameter, $r_{\rm h}$ is a typical dimension (e.g., the radius of a spherical hot spot), and $T_{\rm h}$ is the temperature. The ignition driver must then deliver an energy $E_{\rm ig} = M_{\rm h}CT_{\rm h}$ onto a spot of radius $r_{\rm b} \simeq r_{\rm h}$, in a pulse of duration time $t_{\rm p}$ comparable to the hot spot confinement time $t_c \simeq r_h/c_{\rm sh}$. Here $M_{\rm h}$ is the hot spot mass, C is the DT specific heat, and $c_{\rm sh}$ is the sound speed in DT at temperature $T_{\rm h}$. Since $M_{\rm DT} \propto H_{\rm h}^3/\rho^2$, the parameters of the (delivered) beam scale with the density of the compressed fuel as

$$E_{\rm ig} \propto \frac{1}{\rho^2}; \qquad r_{\rm b} \propto \frac{1}{\rho}; \qquad t_{\rm p} \propto \frac{1}{\rho}; \qquad W_{\rm ig} \propto \frac{1}{\rho}; \qquad I_{\rm ig} \propto \rho. \qquad (4)$$

Here $W_{\rm ig}$ and $I_{\rm ig}$ are, respectively, the delivered power and intensity.

2.1. General pulse requirements

General beam requirements have been determined by a large series of two-dimensional (2D) numerical simulations, where the ignition energy is injected in the form of fast

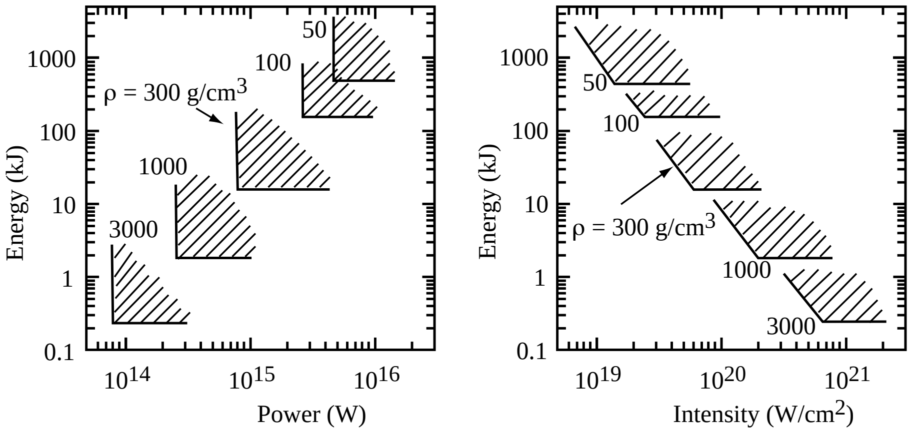

Figure 1. Fast ignition windows, for different values of the fuel density.

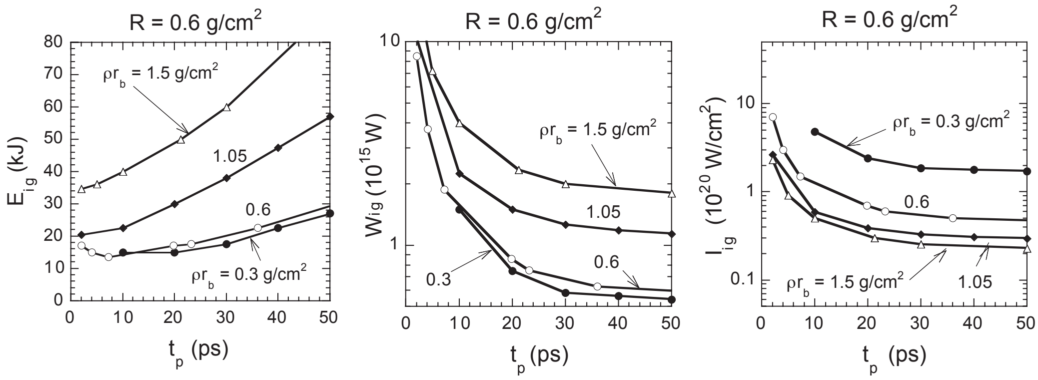

Figure 2. Ignition energy, power, intensity, vs pulse time, for different values of the beam radius, and the same penetration depth $\mathcal{R} = 0.6$ g/cm^2.

particles impinging onto a sphere of precompressed DT. Ignition windows [12, 13] are shown in Fig. 1 for different values of the density. They apply to deposition ranges $0.3 \leq \mathcal{R} \leq 1.2$ g/cm^2. The lower-left-hand side corners of the windows can be identified as optimal pulse parameters, which can be parametrized as a function of the density as [12]

$$E_{ig} = E_{\rm opt} = 140\ \hat{\rho}^{-1.85} \quad \text{kJ}, \tag{5}$$

$$I_{ig} = I_{\rm opt} = 2.4 \times 10^{19}\ \hat{\rho}^{0.95} \quad \text{W/cm}^2, \tag{6}$$

$$W_{ig} = W_{\rm opt} = 2.6 \times 10^{15}\ \hat{\rho}^{-1} \quad \text{W}, \tag{7}$$

$$\tag{8}$$

where $\hat{\rho} = \rho/(100\ \text{g/cm}^3)$. Corresponding pulse duration and focal spot size are

$$t_{\rm p} = t_{\rm opt} = 54\ \hat{\rho}^{-0.85} \quad \text{ps}, \tag{9}$$

$$r_{\rm b} = r_{\rm opt} = 60\ \hat{\rho}^{-0.97} \quad \mu\text{m}. \tag{10}$$

For longer range the required energy increases nearly linearly with $\mathcal{R}$. Using data from the simulations of Ref. [12] (see, e.g. Fig. 2) one finds that Eqs. (5) and (6) can be extended to account also for non-optimal range and focal spot (and still optimal pulse duration) by writing [7]

$$E_{\mathrm{ig}} \geq E_{\mathrm{opt}}(\rho)\ \max(1, \frac{\mathcal{R}}{\mathcal{R}_0}) \times \begin{cases} 1 & r_{\mathrm{b}} \leq r_{\mathrm{opt}}; \\ r_{\mathrm{b}}/r_{\mathrm{opt}} & r_{\mathrm{opt}} \leq r_{\mathrm{b}} \leq 2.5 r_{\mathrm{opt}}; \\ 2.5(r_{\mathrm{b}}/2.5 r_{\mathrm{opt}})^2 & r_{\mathrm{b}} \geq 2.5 r_{\mathrm{opt}}, \end{cases} \quad (11)$$

and

$$I_{\mathrm{ig}} \geq I_{\mathrm{opt}}(\rho)\ \max(1, \frac{\mathcal{R}}{\mathcal{R}_0}) \times \begin{cases} 1 & r_{\mathrm{b}} \leq r_{\mathrm{opt}}; \\ r_{\mathrm{opt}}/r_{\mathrm{b}} & r_{\mathrm{opt}} \leq r_{\mathrm{b}} \leq 2.5 r_{\mathrm{opt}}; \\ 0.4 & r_{\mathrm{b}} \geq 2.5 r_{\mathrm{opt}}, \end{cases} \quad (12)$$

where $\mathcal{R}_0 \simeq 1.2$ g/cm^2.

The simulations of Ref. [12] considered parallel cylindrical beams (with box profiles in radius and time) of unspecified particles with preassigned range, uniform stopping power, and straight path. Computations with more realistic Gaussian profiles lead to energy requirements larger by about 30%. On the other hand, some 2-D simulations also show ignition with energy about 60% of the value of Eq. (5) and (6). This is achieved by exploiting hydrodynamic effects (e.g., shocks, or compression) induced by the absorption of non uniform beams (e.g. a ring-shaped beam) [14] or by the interaction with a suitable mass distribution [15, 16].

Next, we consider ignition requirements for specific drivers.

2.2. Fast ignition by hot electrons

The original, and most widely pursued, fast ignition scheme relies on laser-produced hot electrons. These are created with a nearly-Maxwellian spectrum, with temperature [17]

$$T_{\mathrm{hot}} = \left(\frac{I \hat{\lambda}_{\mathrm{ig}}^2}{1.2 \times 10^{19} \mathrm{W\ cm}^2} \right)^{\frac{1}{2}} \ \mathrm{MeV}, \quad (13)$$

where I is the incident laser intensity and $\hat{\lambda}_{\mathrm{ig}}^2$ is the laser wavelength normalized to 1.06 μm. The average range of such electrons can be approximated as

$$\mathcal{R} = 0.6 f_{\mathcal{R}} T_{\mathrm{hot}} \ \ \mathrm{g/cm}^2, \quad (14)$$

where the parameter $f_{\mathcal{R}}$ ($f_{\mathcal{R}} = 1$ in standard models) has been introduced to account for possible range reduction. For instance, the results of Ref. [18] agree with Eq. (14) with $f_{\mathcal{R}} = 0.5$.

Taking the same radius for both the laser spot size and hot electron spot on the fuel, and using Eqs. (5) and (6) for beam parameters, it can be seen that the range of the hot electrons increases with the compressed fuel density, and may exceed the upper value of the optimal range, $\mathcal{R}_0$. We may compute the required driver energy using Eqs. (11)–(14). For spot radius $r_{\mathrm{b}} \leq 2.5 r_{\mathrm{opt}}$ we get

$$E_{\mathrm{ig}}^{\mathrm{laser}} = E_{\mathrm{ig}}/\eta_{\mathrm{ig}} = \max\left(E_1, E_2\right), \quad (15)$$

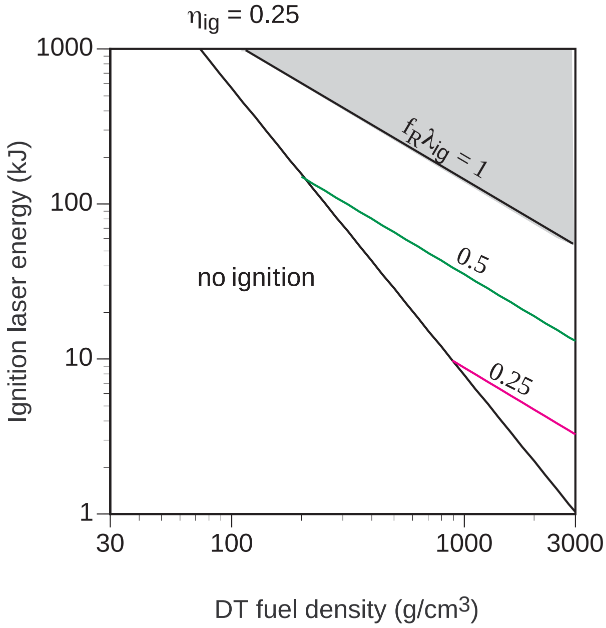

Figure 3. Laser ignition energy for hot-electron driven fast ignition vs density of the precompressed fuel, for different values of the parameter $f_{\mathcal{R}}\hat{\lambda}_{\rm ig}$.

where

$$E_1 = \frac{560}{\hat{\rho}^{1.85}(\eta_{\rm ig}/0.25)} \max\left(1, \frac{r_{\rm b}}{r_{\rm opt}}\right) \qquad \text{kJ}, \tag{16}$$

$$E_2 = \frac{1120}{\hat{\rho}^{0.9}} \left[\frac{1.2}{\mathcal{R}_0} \frac{f_{\mathcal{R}}\hat{\lambda}_{\rm ig}}{(\eta_{\rm ig}/0.25)}\right]^2 \qquad \text{kJ}. \tag{17}$$

(As a reference value, we set $\eta_{\rm ig} = 0.25$, that is the value of the coupling efficiency measured in recent experiments on fast heating of compressed cone-guided targets [19, 20].) Laser energy thresholds vs fuel density are plotted in Fig. 3 for $\eta_{\rm ig} = 0.25$ and different values of $f_{\mathcal{R}}\hat{\lambda}_{\rm ig}$. It appears that the ignition energy can take values well below 100 kJ only for values of $f_{\mathcal{R}}\hat{\lambda}_{\rm ig}$ smaller than one. On the other hand, when $\mathcal{R} > \mathcal{R}_0$ and hence the ignition energy is given by E_2 [Eq.)17)], then $E_{\rm ig}^{\rm laser}$ is independent of $r_{\rm b}$ (for $r_{\rm b} \leq 2.5 r_{\rm opt}$). This relaxes focussing requirements substantially: e.g., for $\rho = 600$ g/cm^3 the required focal spot is $r_{\rm b} \leq 25$ μm, instead of $r_{\rm opt} = 10$ μm.

2.3. Fast ignition by laser-generated protons

Proton induced fast ignition uses a laser-driven proton source placed close to the compressed fuel [2]. In present experiments proton sources have a nearly Maxwellian spectrum. Due to the time-of-flight from source to target the power of the proton beam spreads in time. Simulation results [21] for protons with optimal temperature $T_{\rm p} = 5$ MeV are fitted by

$$E_{\rm ig}^{\rm laser} \simeq \frac{90}{\eta_{\rm ig}\hat{\rho}^{1.3}}[d({\rm mm})]^{0.7} \qquad \text{kJ}, \tag{18}$$

for $1 \leq d \leq 5$ mm. (There is no further advantage in placing the source at distances $d < 1$). This shows that the feasibility of proton fast ignition requires both very small distances d and efficient proton generation.

2.4. Fast ignition by macroparticle impact

Ignition by macro-particle impact has also been proposed. A few years ago, a detailed numerical study [3] concerning gold macroparticles, supported by a simple model, showed that macroparticle velocities of 2000–3000 km/s are required, confirming earlier estimates [22]. Interestingly, the key parameter for ignition is the energy flux (energy per unit area), with a threshold value in good agreement with that computed in a pioneering paper on self-sustained fusion burn-waves [23].

Recently, the scheme has been revived. It has been proposed to use jets generated inside properly shaped laser-irradiated cones [24], or laser-accelerated hollow conical sectors [25], impinging on a precompressed fuel. The viability of such schemes requires both the achievement of ultrahigh velocity and of high density of the impacting projectile.

3. Burn simulations

The burn fraction is usually evaluated as

$$\Phi = \frac{H}{H + H_{\mathrm{B}}}, \tag{19}$$

where $H = \int \rho dr$, averaged over the whole fuel, and $H_{\mathrm{B}} = 7$ g/cm^2. For standard ICF this formula applies for sufficiently large H (see, e.g. [6, 11]) We have now tested it for model fast-ignitor configurations, such as those considered in the ignition studies. The results summarized in Fig. 4 confirm the adequacy of Eq. (19) for systems with H somewhat larger than the particle range and anyhow larger than 1 g/cm^2. There is also a weak dependence on beam intensity.

On the other hand, we have also tested that above such a threshold the burn fraction agrees with Eq.(19), and is independent of the fuel geometry. Finally, it is worth mentioning that some targets, where ignition causes fuel recompression, burn with higher efficiency than predicted by Eq. (19) [15].

4. Gain model and gain curves

4.1. Model

We discuss a model for hot electron-driven fast ignition and laser direct-drive compression. Analogous models describe fast ignitors using indirect compression by either laser drive [7], or heavy ion beams [8]. Simulation-computed gains for various fast ignitor approaches can also be found in the literature [3, 15, 26, 27].

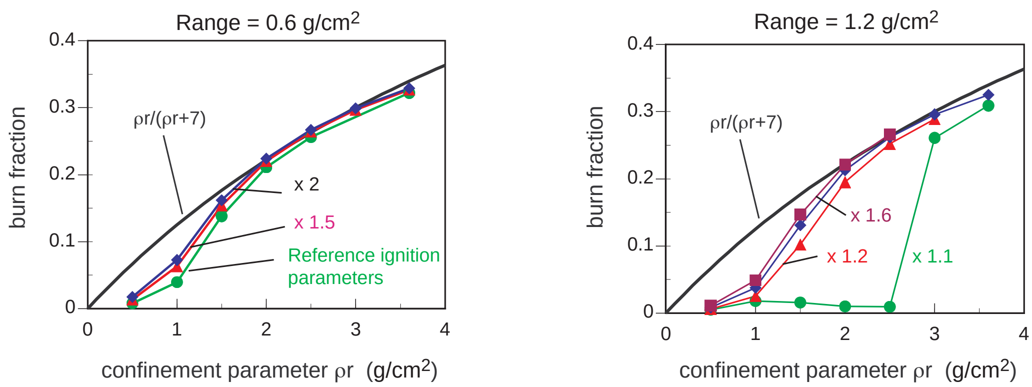

Figure 4. Burn efficiency vs confinement parameter, for different ranges and different ignition pulse parameters.

In our model, the implosion stage is described by a standard model [28]; this yields the in-flight fuel density and pressure, the implosion velocity, the implosion Mach number, and the implosion efficiency as a function of the laser parameters (wavelength λ_c, intensity), in-fligh-aspect ratio (IFAR), and in-flight isentrope parameter. Density, entropy (and then pressure and specific energy) of the stagnating fuel are obtained by a self-similar model [29, 30, 31] as a function of the implosion parameters. The energy of the ignition laser is determined by the model of Sec. 2.

Free parameters of the model are the laser wavelengths, the in-flight-isentrope $\alpha_{\rm ig}$, the laser absorption efficiency $\eta_{\rm a}$, the ignition laser coupling efficiency $\eta_{\rm ig}$, and the range multiplier $f_{\mathcal{R}}$. In the following, we take fixed values of $\alpha_{\rm ig} = 1$, of $\eta_{\rm a} = 0.85$, and of $\lambda_c = 1/3$ μm.

4.2. Gain curves and sensitivity analysis

We summarize and discuss a few important results. More details can be found in Refs. [7] and [8]. A study concerning in particular relatively small driver energy (e.g., 0.5 MJ) will be presented soon [14].

Gain curves $G(E)$, for $f_{\mathcal{R}}\hat{\lambda}_{\rm ig} = 1$, $\eta_{\rm ig} = 0.25$, IFAR limited to 100, and spot size larger than 10 μm are shown in Fig. 5. Gain as large as 500 is achieved at $E = 3$ MJ, for any spot smaller than 50 μm. However, if the ignition laser energy is limited to 100 kJ, gain is only achieved for very tight focussing ($r_b = 10$ μm). For $r_b = 10$ μm, gain $G = 100$ is achieved for total laser energy $E = 300$ kJ. The sensitivy to several model assumptions is illustrated by Table 1, showing the energy required for $G = 100$ under different assumptions. In all cases E is smaller than for conventionally ignited indirect-drive ICF targets.

The gain at the fixed total driver energy $E = 3$ MJ is shown in Fig. 6, as a function of compression laser intensity and IFAR. A large window for high gain at IFAR about

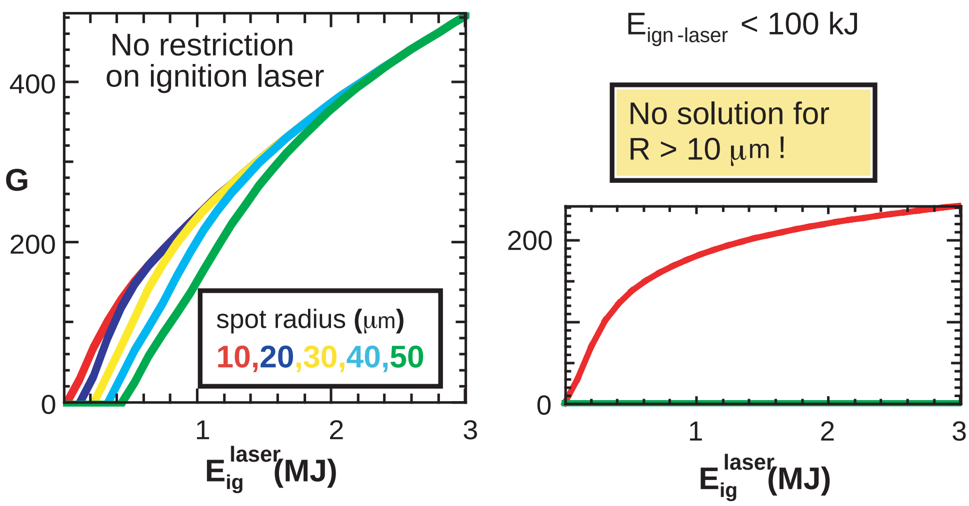

Figure 5. Gain vs total laser energy for different values of the ignition laser spot size, for the parameters given in the main text. a) with no constraints to the ignition laser energy; b) with ignition laser energy limited to 100 kJ.

Model	E (MJ)
mominal	0.3
nominal, but $E_{\mathrm{ig}} \times 0.5$	0.1
nominal, but electron range $\times 3$	0.75
nominal, but $\eta_{\mathrm{ig}} \times 0.25$	1.7

Table 1. Total laser energy required for gain $G = 100$.

50 is found, but this corresponds to large energy of the ignition driver (typically about 0.5 MJ [8]).

Current experiments show that electrons spread over spots of 20 μm or larger. Achieving ignition and gain with a spot of 20 μm and ignition laser of less than 100 kJ requires values of $f_{\mathcal{R}}\hat{\lambda}_{\mathrm{ig}}$ of 0.5 or smaller, i.e. either a short wavelength ignition laser or some reduction to the range of the hot electrons. Gain contours for $f_{\mathcal{R}}\hat{\lambda}_{\mathrm{ig}} = 0.5$, $E = 0.5$ MJ and $r_b \geq 20$ μm are shown in Fig. 7. It is seen that a window exists for gain $G > 100$ with IFAR about 50.

5. Conclusions

The gain curves discussed above confirm the potential of fast ignition for high gain. However, the curves also show critical dependencies on the focal spot radius and on the coupling efficiency of the ignition laser. The latter, involving hot electron generation and transport to the compressed fuel, is a key issue for fast ignition. Hot electrons parameters, such as temperature and range also play a crucial role. All these aspects

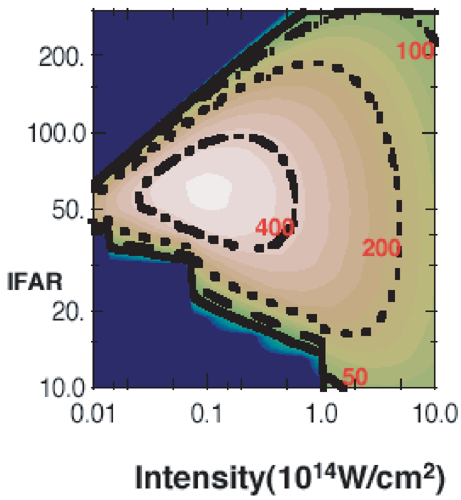

Figure 6. Gain contours in the IFAR-compression laser intensity plane, for total laser energy of 3MJ; focal spot limited to 10 μm; $f_{\mathcal{R}}\hat{\lambda}_{\mathrm{ig}} = 1$.

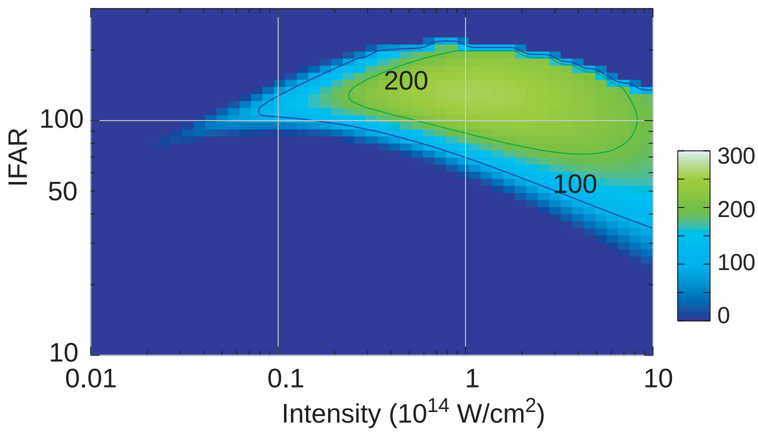

Figure 7. Same as Fig. 6, but for total laser energy of 500 kJ, focal spot limited to 20 μ, and $f_{\mathcal{R}}\hat{\lambda}_{\mathrm{ig}} = 0.5$.

deserve experiments.

A more quantitative appraisal of the ignition requirements could be achieved by simulations including more realistic descriptions of both particle beam and compressed fuel. Concerning the compression stage, relevant information could be provided by scaled-down experiments, that can already be performed at existing facilities.

Acknowledgments

S. A. thanks A. Schiavi and C. Bellei for their help in running 2D numerical simulations and the gain model. The participation of S.A. in the 2005 Fast Ignition Workshop was supported by the ESF COST project P-14.

References

[1] Tabak M *et al* 1994 *Phys. Plasmas* **1** 1626
[2] Roth M et al 2001 *Phys. Rev. Lett.* **86** 436
[3] Caruso A and Pais V A 1996 *Nucl. Fusion* **36** 745
[4] Basko M M, Churazov M D and Aksenov A G 2002 *Laser Part. Beams* **20** 411
[5] Tabak M *et al* 2005 *Phys. Plasmas* **12** 057305
[6] Atzeni S and Meyer-ter-Vehn J 2004 *The Physics of Inertial Fusion* (Oxford: Clarendon)
[7] Tabak M, Atzeni S, Campbell M H, and Tanaka K 2005, Introduction to the Fast Ignitor *Fusion Sci. Techn.*, in press.
[8] Tabak M and Callahan D 2005 *Nucl. Instr. Meth. A* **554** 48
[9] Nakai S and Mima M 2004 *Rep. Progr. Phys.* **67** 321
[10] Key M *et al* 1999, Progressin Fast Ignition Research Using the NOVA Petawatt Laser, in *Fusion Energy 98*, (IAEA: Vienna) 1098
[11] Atzeni S 1995 Jpn. J. Appl. Phys. **34** 1980
[12] Atzeni S 1999, Phys. Plasmas **6** 3316
[13] Atzeni S 2000, Improved studies on the ignition requirements for DT and T-poor fast ignitors, in Inertial Fusion Sciences and Applications 99 (ed. by C. Labaune *et al*) (Paris: Elsevier), p. 415
[14] Atzeni S, Bellei C, Schiavi A 2005, to be published
[15] Hatchett S, Tabak M, Turner R and Stephens R 2001, New Developments in Design of Cone-Focused Fast Ignition Targets, in Proceedings of 5th Workshop of Fast Ignition of Fusion Targets, Madeira, June 2001, paper W.18.
[16] Herrmann M, Hatchett S and Tabak M, Reducing ignitor energy for fast ignition by controlling energy deposition, APS 2001, paper FO2.013.
[17] Wilks S C, Kruer W L, Tabak M and Langdon A B 1993 *Phys. Rev. Lett.* **69** 1383
[18] Deutsch C *el al.* 1996 *Phys. Rev. Lett.* **77** 2483
[19] Kodama R. *el al.* 2001 *Nature (London)* **412** 798
[20] Kodama R. *el al.* 2002 *Nature (London)* **418** 933
[21] Atzeni S, Temporal M and Honrubia J H 2002 *Nucl. Fusion* **42** L1
[22] Harrison F R 1963 *Phys. Rev. Lett.* **11** 535
[23] Chu M S 1972 *Phys. Fluids* **15** 413
[24] Velarde P *et al* 2005 *Nucl. Instr. Meth. A* **554** 554
[25] Murakami M and Nagatomo H 2005 *Nucl. Instr. Meth. A* **554** 67
[26] Temporal M, Honrubia J H and Atzeni S 2002 *Phys. Plasmas* **9** 3098
[27] Ramis R and Ramirez J 2004 *Nucl. Fusion* **44** 720
[28] Lindl J D 1997 *Inertial Confinement Fusion: The Quest for Ignition and High Gain Using Indirect Drive* (New York: Springer)
[29] Meyer-ter-Vehn J and Schalk C 1982 Z. Naturforsch. **37a** 302
[30] Kemp A, Meyer-ter-Vehn J and Atzeni S 2001 *Phys. Rev. Lett.* **86** 3336
[31] Hermann M C, Tabak M and Lindl J 2001 *Nucl. Fusion* **41** 99

This work was performed under the auspices of the U.S. Department of Energy by University of California, Lawrence Livermore National Laboratory under contract W-7405-Eng-48.